Cavitation erosion in liquid nitrogen

Matevž Dular, Martin Petkovšek

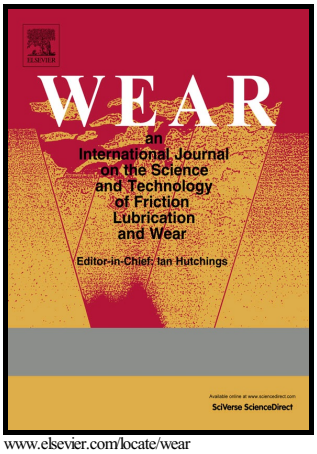

www.elsevier.com/locate/wear

PII: S0043-1648(17)31139-0
DOI: https://doi.org/10.1016/j.wear.2018.01.003
Reference: WEA102335

To appear in: *Wear*

Received date: 17 July 2017
Revised date: 3 January 2018
Accepted date: 3 January 2018

Cite this article as: Matevž Dular and Martin Petkovšek, Cavitation erosion in liquid nitrogen, *Wear,* https://doi.org/10.1016/j.wear.2018.01.003

Cavitation erosion in liquid nitrogen

Matevž Dular (corresponding author)
Laboratory for Water and Turbine Machines
Faculty of Mechanical Engineering
University of Ljubljana
Askerceva 6, 1000 Ljubljana, SI-Slovenia
E-mail: matevz.dular@fs.uni-lj.si
Phone: +386 1 4771 453
Fax: +386 1 2518 567

Martin Petkovšek
Laboratory for Water and Turbine Machines
Faculty of Mechanical Engineering
University of Ljubljana
Askerceva 6, 1000 Ljubljana, SI-Slovenia

Abstract
Thermodynamic effects in cavitation become significant only when the critical-point temperature is close to the operating temperature of the fluid, as in the case of cryogenic fluids. Therefore, the understanding and the prediction of the cavitation effects in such cases is crucial in many applications - for example the turbopumps for liquid hydrogen (LH2) and oxygen (LOX) in space launcher engines. The new generation of rocket engines will also feature the possibility of re-ignition while in orbit and prolonged period of operation; hence cavitation erosion is becoming an issue at the design stage of the turbo-pumps.
In the study, we show measurements of cavitation erosion in liquid nitrogen (LN2), where cavitation was generated by an ultrasonic transducer. The damage was evaluated on aluminium samples. Special care was given to accurate setting of the operation point – especially the operating pressure, which defines the size of cavitation. We show that it is less aggressive than cavitation in water and that its aggressiveness cannot be described by a single fluid property (for example the most commonly used Brennen's thermodynamic parameter Σ), but by a combination of several (viscosity, density, vapor pressure, surface tension, thermodynamic parameter) – in the present paper we addressed this point by a simple bubble dynamics model with consideration of the thermodynamic effect to qualitatively predict the results of the measurements. Finally, we also compared performance of several other engineering materials.

Key words: Caviation; Erosion; Liquid Nitrogen; Thermodynamic effect

1 Introduction

Optimal operation of turbopumps is crucial for all liquid fuel rocket engines. To reduce weight, these pumps often operate at critical conditions, where dynamic instability and cavitation are unavoidable. In cryogenic engines, the fuel and oxidizer used are liquid usually hydrogen and liquid oxygen at very low temperatures (about 14 and 90 K, respectively). Usually we treat cavitation as an isothermal phenomenon, but this assumption is not valid for such propellants: flows are characterized by a substantial cooling during the vaporization process due to cavitation. This phenomenon delays the further development of cavitation, so it plays a moderation role in

the growth of cavitation bubbles. The numerical prediction of the thermal effect is therefore a major industrial issue. Similarly, a more in-deep understanding of cavitation erosion is extremely important for future reusable components, designed in order to withstand longer lifetimes without suffering potentially dangerous damages.

Many studies were already performed to investigate these phenomena [1]–[5], yet, due to the complexity of the measurements, most avoid experiments in cryogenic fluids. Despite the progress in the recent years, Hord's extensive experimental studies [6]–[8] □in the 1970's are still considered as a benchmark for validating numerical models with thermodynamic effects consideration. First experimental study by direct, non-invasive temperature measurement method on single bubble was performed much later by [2]. First 2D temperature fields of the cavitating flow in hot water, measured on Venturi constriction were performed by the present authors [9], [10].
The lack of experimental data is especially evident for the case of cavitation erosion problem where sometimes very long test are required.
The effects of medium temperature on the aggressiveness of cavitation erosion were studied already by Garcia & Hammitt [11], Young & Johnston [12]and Plesset [13] conducted vibratory tests. Although valuable, the main issue that is common for their studies is that they did not consider the fact that also the system pressure needs to be raised to achieve comparable cavitation extent at higher medium temperature. The same goes to a more recent study by Hattori [14]. The effect of water temperature, with rigorous control of the cavitation number, was recently investigated for the case of hydrodynamic cavitation by the present author [15]. Cavitation erosion in cryogenic fluids was not yet investigated under a rigorous control of the pressure and consequently under control of cavitation extent and its dynamics.

In the present study, we first show the design of the facility where also the system pressure can be adjusted. Then results of erosion measurements in LN2, which is the core of the paper, are presented. We also give comparison of these results to the tests in water at low and high temperature and the results of damage evaluation on other engineering materials (again in LN2). Finally, we employed a model which we derived in the study of temperature effect in water [15] and show that it can qualitatively predict the effect seen in the experiments.

2 Experiment

Experiments were performed in the CryoCav experimental facility (European Space Agency) at the Department for Power Engineering, Faculty of Mechanical Engineering, University of Ljubljana, Slovenia.

2.1 Experimental set-up

The core of the setup is a ultrasonic homogenizer Cole-Parmer 750W, with a nominal output frequency f_0=20000 Hz. Titanium horn diameter was submerged 20 mm in a closed vessel (pressure chamber), specially designed to operate at cryogenic temperatures (Fig. 1). Sufficient submergence prevented the interaction of the horn tip and the free surface. Insulated vessel is used to contain the cryogenic liquid and to lengthen its state in the liquid phase. The vessel enables the variation of ambient pressure by which different intensities of cavitation can be achieved. Moreover, the evaporation rate of the liquid can be minimized. As the pressure increases due to constant evaporation a precise regulation valve is mounted to maintain constant

pressure conditions. In addition, an automatic safety valve is installed for quick pressure release. Temperature inside the vessel was monitored by a Pt100 probe, mounted below the observation and illumination window through which cavitation could be observed by a high-speed camera. The static pressure inside the chamber was monitored by electronic Endress&Hauser gauge pressure sensor and pressure Bourdon tube.

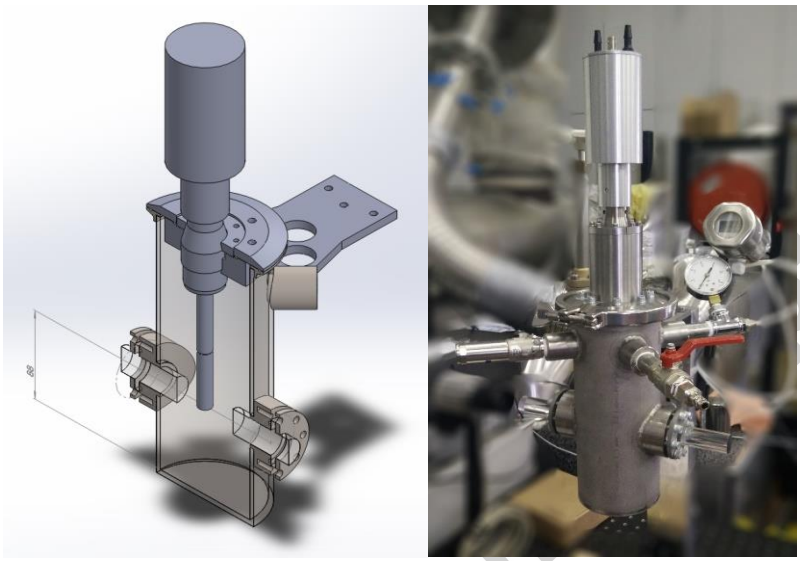

Figure 1: Experimental set-up (without insulation).

2.2 Specimens and damage evaluation

For the present study, most of the specimens were made out of Aluminum 6060. Other materials were also investigated (see section 3.4). The face of the specimens was polished. An example of fresh specimen, specimen after short (pits only) and after long exposure (mass loss) to cavitation is shown in Fig. 2.

Figure 2: Dimensions of the specimen and its appearance prior and post exposure (pits only and mass loss) to cavitation.

The specimens were mounted to the ultrasonic horn – the test was conducted in "direct mode" without a stationary specimen. This was necessary since relatively low erosion rate was expected and the direct mode measurements are known to be more aggressive [16], [17].

After the exposure to cavitation the specimen was photographed by a Canon D3200 camera with fitted infinity Proximity InfiniTube and an additional Mitutoyo lens. To photograph the entire surface of the specimen 4 to 8 photographs of different sub-areas were taken. At this resolution the pixel size in the image corresponded to about 3 μm.

The question of which material parameter is the most important one when describing its resistance to cavitation erosion is not an easy one. In the present study we measured the surface hardness of the material, mainly because the majority of the tests were conducted during the incubation period (no mass loss), where other material effects (work hardening, fatigue etc.) are not yet significant. The surface hardness of the alloy was measured at different temperatures. For high temperature the specimen was put into boiling water (100°C) and left to cool down to 90°C. For low temperature it was submerged into LN2. A standard static Brinell test (HBW 1/10) [18] with a 1mm ball diameter, force of 10 kg (98.07 N) and duration of 10 s was used. The temperature of the specimen did not change significantly during the test – it was monitored by a IR thermometer. It was found that the material gets somewhat harder when it is cooled down to -196°C and the hardness remains almost the same at an increased temperature – HB=60 (20°C), HB=56 (90°C), HB=70 (-196°C).

The evaluation followed a well established pit-counting technique [7, 10], where we recognize pits as the darker regions in an image, while the brighter area is assumed to be undamaged surface. The pit-count method gives a distribution of the number and the area of the pits and consequently, the distribution of the magnitude of cavitation erosion on the surface. The measured damaged area is also in good correlation with the volume of the deformed material [19]. In this paper we give the ration between the damaged surface and the evaluated surface (in percentage) as a measure of the damage:

$$Damage = \frac{Damaged\ Area}{Evalueted\ Area} \cdot 100\% \,. \qquad (1)$$

The evaluated are in the present experiments was approximately 100 mm^2.

For the mass loss tests the specimens were weighted prior to the exposure to cavitation and several times during the length of the experiment. A precision scale Sartorius MC 210 S with resolution of 0.01 mg was used.

2.3 Acoustic cavitation number definition

Up to today, no consensus on the so-called cavitation number in acoustic cavitation exists. A single nondimensional number, which would, at least approximately, define the extent of the cavitation is hard to define and requires a vast experimental campaign. This is an endeavour of our future research and does not fall in the scope of the present paper. Nevertheless, we propose a new way to define a nondimensionalized cavitation parameter, which includes the energy potential that needs to be reached to achieve evaporation ($p_\infty - p_v$) and the energy delivered by the ultrasonic horn. The derivation of the parameter begins with the hydrodynamic cavitation number:

$$\sigma = \frac{(p_\infty - p_v)}{\frac{1}{2}\rho v^2} \qquad (2)$$

where p_∞ is the system pressure, p_v is the vapour pressure, ρ is the density of the fluid and v is the velocity. All parameters except the latter are easily determined. For the velocity one should take the maximal velocity of the horn (v_{max}), which is related to its power (P). From the equation for the impedance (Z) one gets:

$$Z = \frac{p}{\bar{v}} = \rho c \xrightarrow{yields} p = \rho c \bar{v}, \quad (3)$$

where p is pressure, $\bar{v}$ is the average velocity of the horn, ρ is the liquid density and c is the sonic velocity in the liquid. If we combine Eqn. 3 with the one for intensity, we get:

$$I = \frac{P}{A} = p\bar{v} = \rho c \bar{v}^2, \quad (4)$$

Where I is the intensity and A is the horn tip area. The average velocity of the horn is then:

$$\bar{v} = \sqrt{\frac{P}{A\rho c}} \quad (5)$$

Finally, considering a sinusoidal movement of the horn with a known frequency we get the maximal velocity:

$$v_{max} = \frac{\bar{v} t_0 \omega}{-\cos(\omega t_0)} = -\sqrt{\frac{P}{A\rho c}} \frac{t_0 \omega}{\cos(\omega t_0)}, \quad (6)$$

where ω is the horn frequency ($\omega = 2\pi f$) and t_0 is the half time of the period ($t_0 = \frac{1}{2f}$) – the time the horn needs to reach maximal velocity. Finally, we introduce the velocity v_{max} as the velocity into to Eqn. 2 to calculate the acoustic cavitation number:

$$\sigma = 2(p_\infty - p_v) \frac{Ac}{P} \left(\frac{\cos(\omega t_0)}{\omega t_0} \right)^2. \quad (7)$$

In theory, the same value of cavitation number (regardless of the value of individual variables) should result in the same extent of the cavity.

A snapshot (the first line) and the time averaged appearance (the second line) of cavitation on the horn at different cavitation numbers are shown in Fig. 3. These correspond to the investigated cavitation conditions in this study. Cavitation in cold and hot water and in LN2 is compared at a constant σ value. In addition, cavitation in LN2 at various σ values, which correspond to the investigated cavitation conditions in this study, are shown.

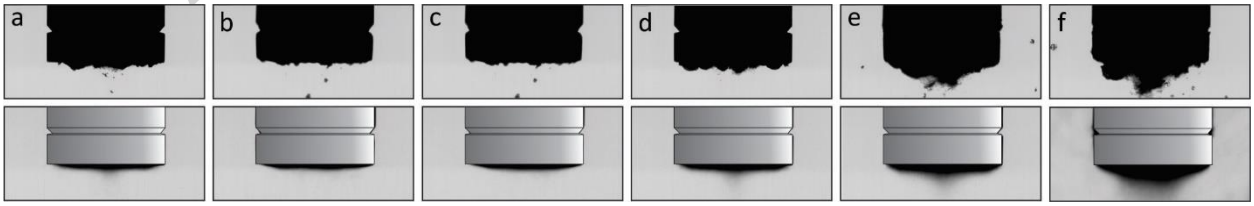

Figure 3: Cavitation in cold water (20°C) (a), hot water (90°C) (b), in LN2 (c) at σ=9 and in LN2 at σ =6.8 (d), 4.5 (e) and 2.3 (f). All at transducer power P=338W.

As we can see the appearance of cavitation at a constant σ value is similar – regardless of the fluid (a, b and c). As the cavitation number is reduced (from c to f), the cavitation grows and

covers the entire tip of the horn (e and more clearly f) – we enter the condition of acoustic supercavitation, which resembles the one on a smaller, 3mm, horn tip [20]. When one calculates the acoustic cavitation number (Eqn. 7) for the acoustic supercavitation conditions, published in [20] one gets σ=4.2. A similar value of σ in both studies (regardless of the specifics of both experiments – fluid, diameter, temperature) confirms that we are dealing with the same cavitating conditions.
We can conclude that for the purpose of the present investigation the described derivation of the acoustic cavitation number is valid, but a much more detailed study of this parameter is to be performed and is planned in the future to ensure valid comparison across the scales.

The peak to peak frequencies were measured from the images taken by a high-speed camera. The uncertainty of these measurements was considerable (±1 pixel or ±10μm); hence the values can only be taken as an orientation. These are given in Tab. 1.

2.4 Investigated conditions
The experiment was designed in a way to compare erosion at the same values of cavitation number σ, while other variables were varied. Table 1 shows the investigated conditions (T…liquid temperature, ρ… liquid density, p_∞…system pressure, p_v…vapour pressure, P… ultrasonic transducer power, Amp… horn peak to peak amplitude, σ…cavitation number).

Table 1: Investigated conditions

	Fluid	T (°C)	ρ (kg/m^3)	p_∞ (kPa)	p_v (kPa)	P (W)	Amp (μm)	σ (-)
1	LN2	-195.8	807	125	100	225	89	2.3
2	LN2	-195.8	807	150	100	225	85	4.5
3	LN2	-195.8	807	175	100	225	79	6.8
4	LN2	-195.8	807	200	100	225	89	9.0
5	LN2	-195.8	807	138	100	338	98	2.3
6	LN2	-195.8	807	175	100	338	103	4.5
7	LN2	-195.8	807	213	100	338	103	6.8
8	LN2	-195.8	807	250	100	338	111	9.0
9	LN2	-195.8	807	150	100	450	126	2.3
10	LN2	-195.8	807	200	100	450	112	4.5
11	LN2	-195.8	807	250	100	450	120	6.8
12	LN2	-195.8	807	300	100	450	116	9.0
13	H2O	20	998.2	109	2.3	338	77	9.0
14	H2O	90	965.3	172	70	338	81	9.0

In all 14 operating points were investigated – 12 in liquid nitrogen at cryogenic temperature and two additional tests in cold and hot water, which served as a reference. Each experimental condition was investigated 5 times to ensure repeatability of the measurements.

To ensure repeatable measurements we had to degas the liquids prior to the tests – it is known that the presence of non-condensable gasses significantly influences the cavitation

aggressiveness [21]. For the case of LN2 this was achieved by default as it was stored at near boiling state at 1 bar. As for the water at 20°C, it was carefully prepared. Firstly, a distilled water was always used. Its temperature was then raised to boiling and left there for 10 minutes. It was then poured to the cavitation chamber and left to cool down to 20°C. Afterwards the system pressure was lowered, to again reduce the presence of the gasses. After this the water gas content was reduced to the minimum possible level, which should be comparable to the one of the LN2. Similarly, for the hot water experiments at 90°C, the distilled water was first boiled (at 1 bar) and then poured to the chamber to cool down. No degassing was needed in this case due to the much shorter time of cooling.
Since the liquids were degassed, the nuclei that contributed to the first appearance of cavitation, were likely introduced by the ultrasonic horn tip itself – micro size gas (air) pockets attached to its imperfect surface.

Even though comparable conditions in respect to the non-condensable gas content were achieved for all three fluids, a question on the composition non-condensable gases in LN2 remains open. A detailed investigation of this lies outside the scope of the present work, but is likely that H_2 and He, which both have saturation temperature lower than the one of N_2, take this role.

Damage on the specimen was evaluated before the exposure to cavitation and then after 12, 24, 36, 48 and 60 seconds of exposure. In addition, tests with longer exposure time were performed to study mass loss.

3 Results

First the results at the same ultrasonic horn power and different cavitation numbers are compared. A comparison of the influence of the horn power (at constant cavitation numbers) follows. Results of tests in cold and hot water are then given for the sake of a reference and discussion on the influence of thermodynamic delay on the cavitation aggressiveness. After the presentation of the mass loss tests the results of comparison of different materials are finally given.

3.1 Influence of the cavitation extent

Figure 4 shows the specimens after a 60 second exposure to cavitation at horn power P=338W, for four cavitation numbers (σ = 2.3, 4.5, 6.8 and 9).

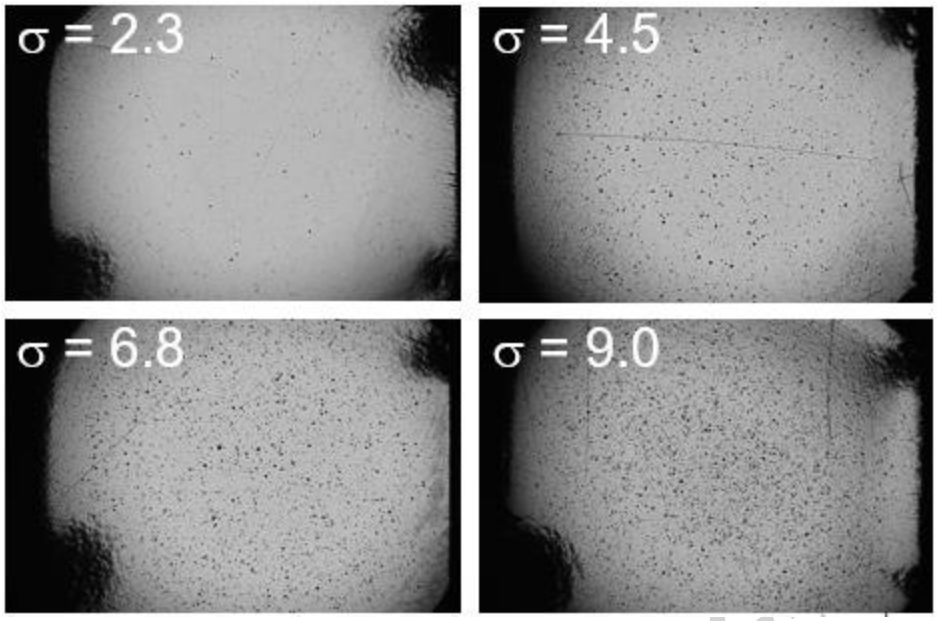

Figure 5: Damage to the specimen after 60 second at different cavitation numbers and the same power (338W).

From Fig. 5 one can see that cavitation damage obviously increases with increasing cavitation number. The final extent of damage was 0.53, 1.12, 5,87 and 8.99% for σ=2.3, 4.5, 6.8 and 9.0, respectively. The damage at the perimeter of the specimen is not related to cavitation – it was sustained at the screwing/unscrewing of the specimen.

More interesting is the quantitative data shown in diagrams in Fig. 6 where we show the evolution of the damage accumulation at horn powers P=225, 338 and 450 W, for four cavitation numbers (σ = 2.3, 4.5, 6.8 and 9).

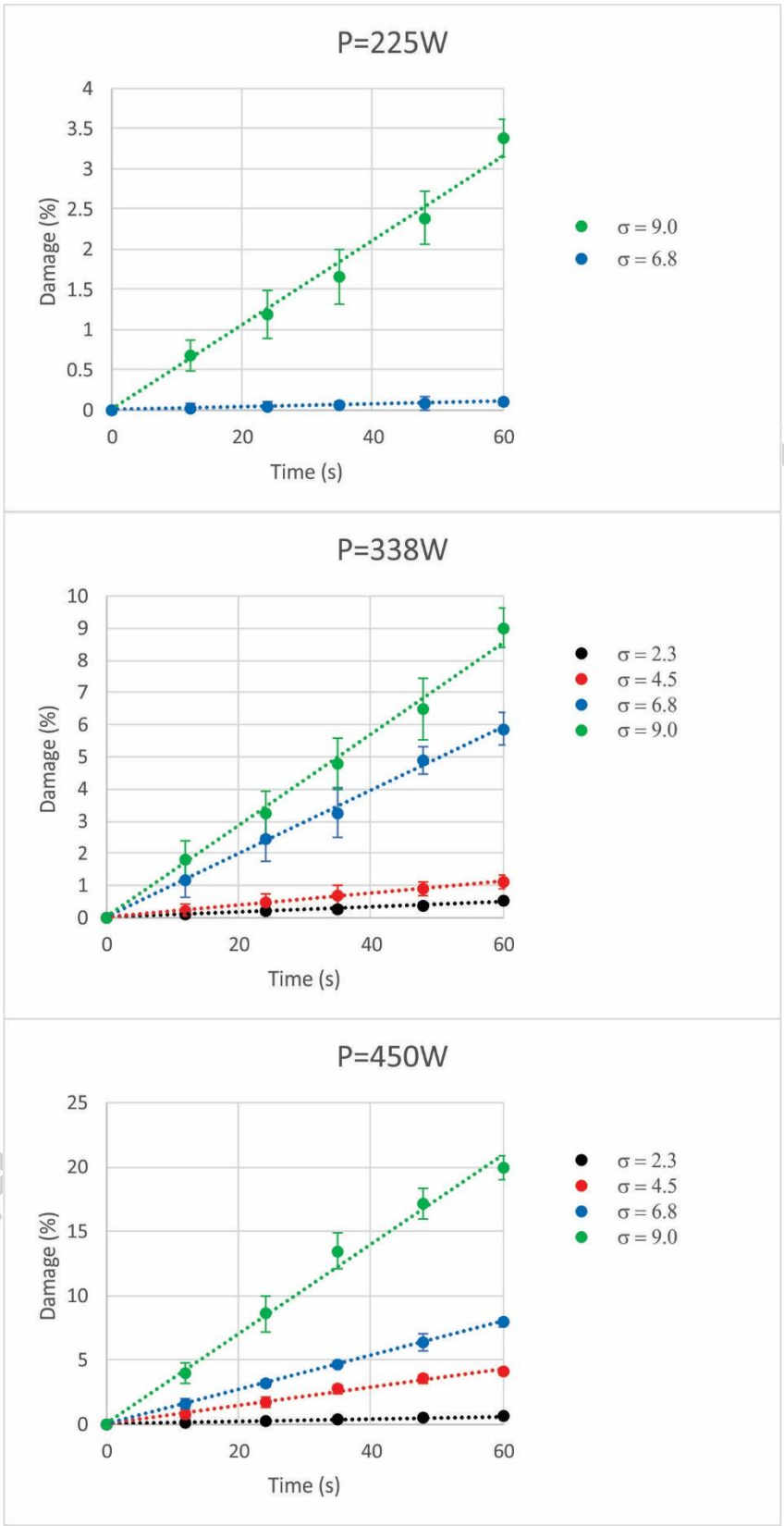

Figure 5: Damage evolution at P=225, 338 and 450 W and different cavitation numbers (σ = 2.3, 4.5, 6.8 and 9).

The trend is the same for all three investigated powers. In the case of the lowest one (225 W) no damage could be detected at σ=2.3 and σ=4.5, which are the least aggressive conditions at higher transducer powers also. In general, the cavitation aggressiveness increases as the cavitation number increases. This seems to be contradictory to the general opinion that larger cavity will be more aggressive. However, in the present case we are dealing with conditions at which an attached cavity is transitioning to a supercavity (see also Fig. 3), and the latter is known to be less aggressive [22], since it engulfs the entire solid body and does not collapse on it [23]. Cavitation at σ=9 roughly corresponds to the extent of the cavity at a standard G32 test [16], which is designed to produce very aggressive type of attached cavitation.

3.2 Influence of the power of the transducer

For the ease of discussion, the results are presented again, but this time according to the power of the transducer. Figure 6 shows the specimens after a 60 second exposure to cavitation at σ = 9 for three different horn powers (P=225, 338 and 450 W).

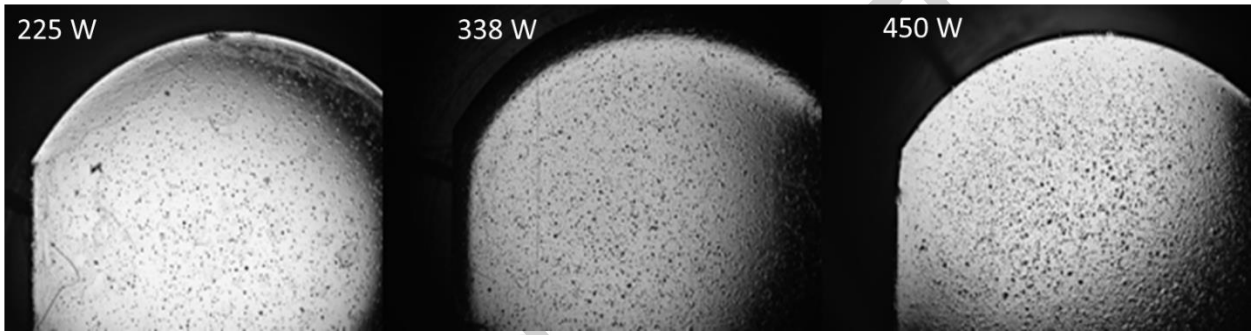

Figure 6: Damage to the specimen at different powers and the same cavitation number (σ=9).

As one can see the aggressiveness increases significantly when the transducer power increases (at a constant cavitation number (and size of cavitation)).

Again, one can appreciate more the quantitative data for all the investigated cavitation numbers, shown in Fig. 7.

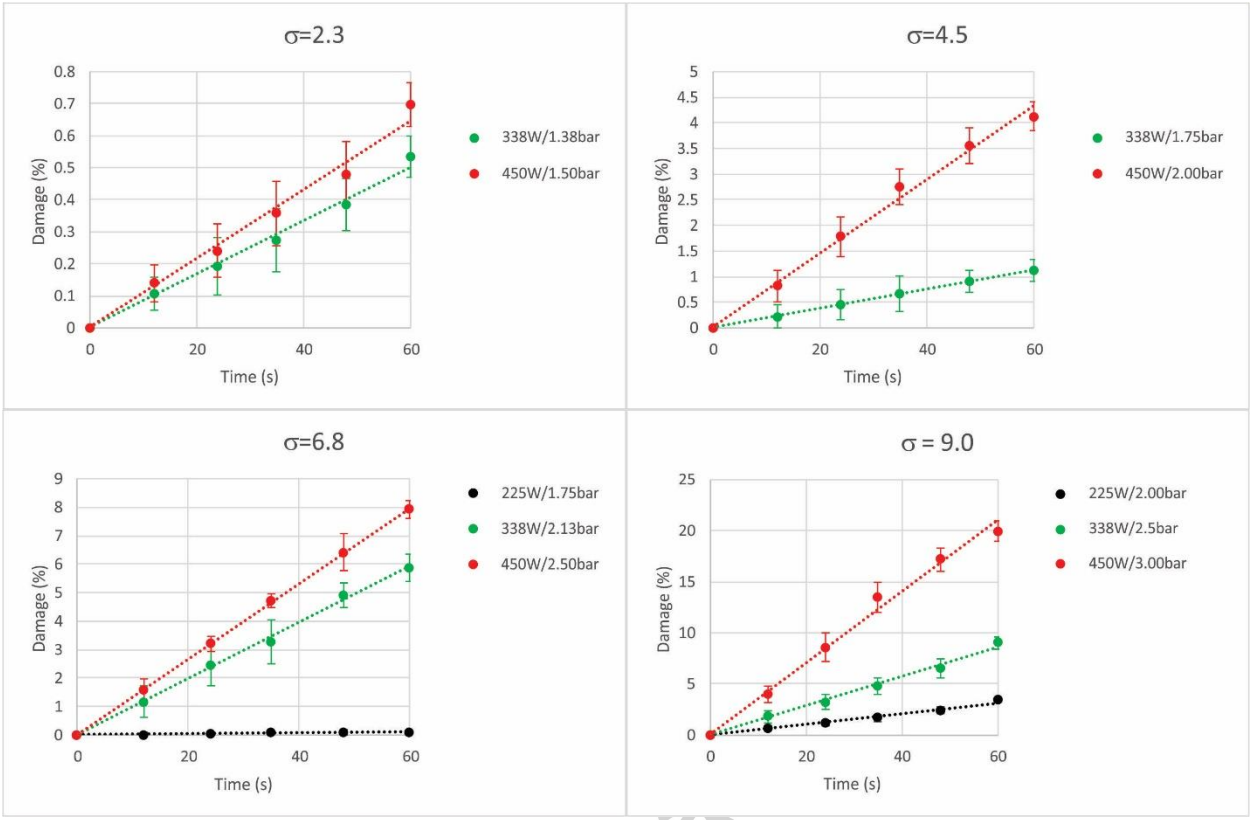

Figure 7: Damage evolution at σ = 2.3, 4.5, 6.8 and 9P=225, 338 and 450 and different horn powers (P=225, 338 and 450 W).

Again, the trend of increasing the cavitation aggressiveness with increasing transducer power can be seen for all the investigated conditions. No damage was detected at the lowest power and lower σ values.

Interestingly the damage follows a well know power low pattern – the extent increases with a power law as the power (velocity) of the horn is increased. The velocity of the horn tip is closely related to the power of the transducer (see Eqns. 5 and 6). A power law is usually obtained in cavitation erosion studies [21]:

$$\frac{ER_{v1}}{ER_{v2}} = \left(\frac{v1}{v2}\right)^{n}, \quad (8)$$

where ER_{v1} and ER_{v2} represent the erosion rates at corresponding flow velocities v_1 and v_2, respectively. n usually lies in the range between 4 and 8. A value of n=7.8 was determined from the experiments, what complies with measurements in water and hydrodynamic cavitation.

3.3 Comparison to cavitation in cold and hot water

As we approach the critical temperature of the liquid the densities of the liquid and vapor become more similar. In a result, evaporation requires more latent heat what results in a phenomenon known as "thermal delay". Cavitation cannot be treated as an isothermal phenomenon since the latent heat flow from the liquid to the vapor results in a local decrease of

temperature of the bulk liquid. The parameter that defines the sensitivity of the liquid to the thermal delay phenomenon was introduced by Brennen [23]:

$$\Sigma = \frac{(\rho_v L)^2}{\rho_l^2 c_{p,l} T_\infty \sqrt{\alpha_l}} \ , \qquad (9)$$

where T_∞ is the test temperature, ρ_v is the vapor density, ρ_l is the liquid density, L is the evaporative latent heat, c_{pl} is the constant pressure specific heat of the liquid and α_l is the thermal diffusivity of the liquid. For the present experiments, the values of Σ are $4ms^{-3/2}$, $1602ms^{-3/2}$ and $1925ms^{-3/2}$ for cold water 20°C, hot water 90°C and LN2, respectively.

The experiment was terminated after the maximal pit number density, where optical evaluation is still possible, was achieved. Figure 8 shows the specimen after the conclusion of the experiment. The length of the test had to be adjusted, as the erosion rate in water was considerably higher than in LN2.

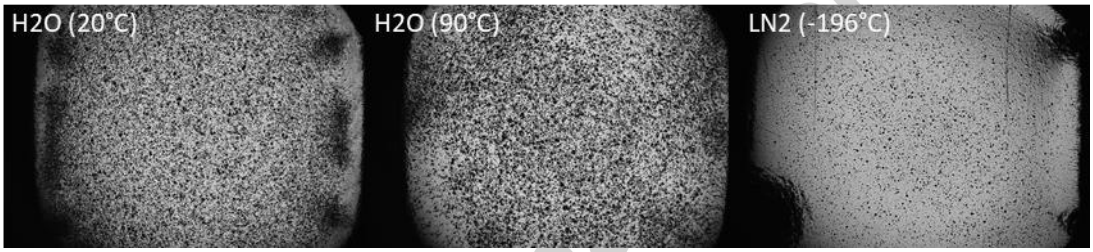

Figure 8: Specimen after the end of experiment in water at 20°C (left) (0.6s), water at 90°C (middle) (1.2s) and in LN2 (right) (60s), to and to. At P=338 W and σ=9.

Obviously, cavitation in water is significantly more aggressive (regardless of its temperature) than in LN2. The sustained damage after only 0.6 or 1.2s of exposure was on the limit of the capability of the software to recognize the individual pits, hence the experiment needed to be stopped much faster than anticipated.

Figure 9 gives the quantitative comparison of cavitation aggressiveness in the three liquids.

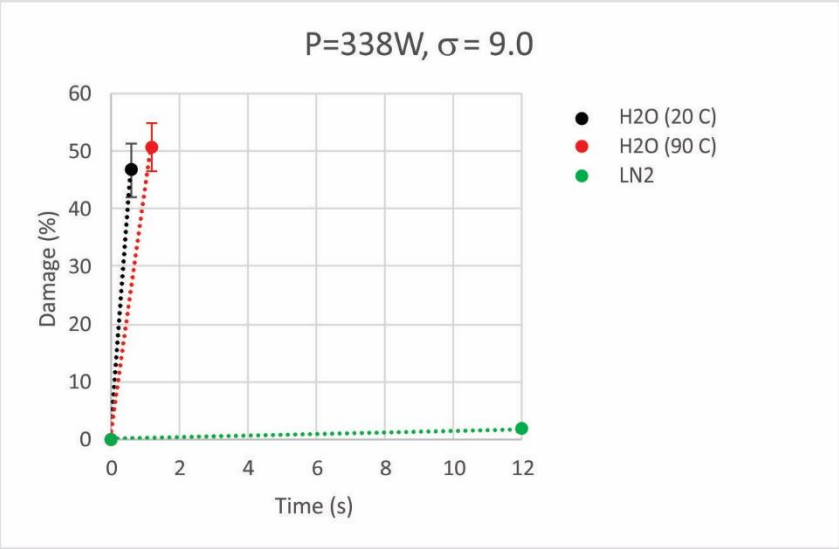

Figure 9: Damage evolution at cavitation number σ=9.0, P=338W for LN2, cold (20°C) and hot (90°C) water.

Only the data for the 12 s exposure is shown for the case of LN2 for the sake of easier comparison. Unexpectedly the cavitation in LN2 was found to be less aggressive – even when compared to the one in hot water. This puts into a question the Σ parameter and the use of hot water as a surrogate fluid in studies of thermal effects of cavitation.
Another, similar, conclusion can be drawn from the interesting point that cavitation damage rate in hot and cold water is almost the same. This was at first not anticipated since Σ values are very different and thermal effects should play a decisive role. But when one considers the past studies of cavitation erosion in waters with different temperatures [3], [14], [24] a clear pattern where a maximal erosion rate is found at about 50-70°C can be seen. Also the erosion rates at 20°C and 90°C are reported to be comparable. This again puts a question to the exclusive use of Σ as a parameter that defines cavitation aggressiveness.

3.3.1 Mass loss measurements

In the scope of comparison of the erosion rates in LN2 and water at different temperatures also mass loss test were performed, which revealed the same trend (Fig. 10).

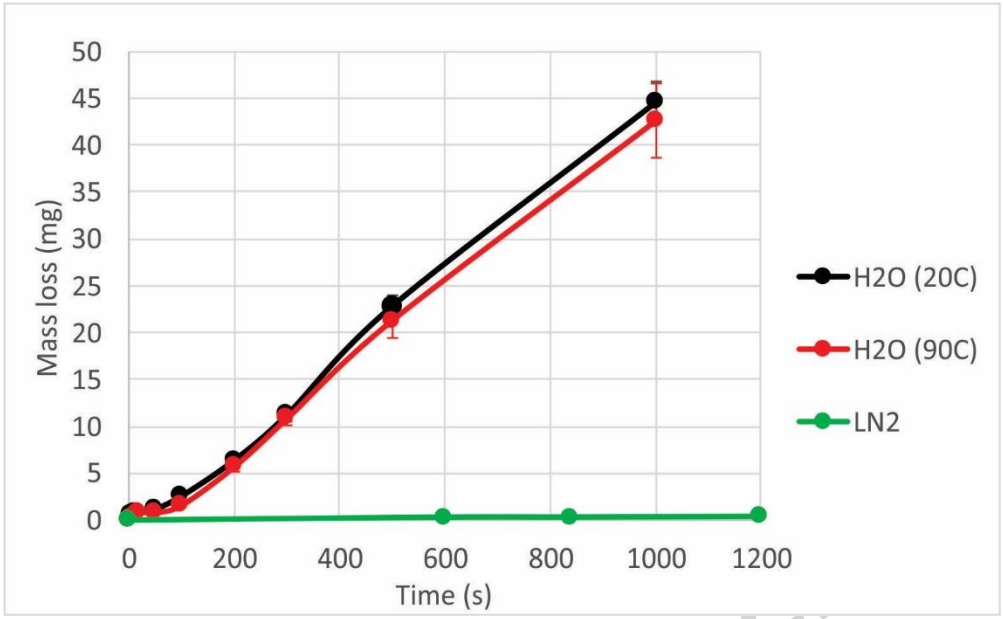

Figure 10: Mass loss at cavitation number σ=9.0, P=338W for LN2, cold (20°C) and hot (90°C) water.

Results of mass loss test confirm the trends, which were determined from the studies in the incubation period. While the mass loss follows a well know incubation-acceleration-steady state trend for the case of water (both at 20 and 90°C) almost no material loss was measured in the case of LN2 – even if we prolonged the test. After 1200 seconds only 0.31 mg decrease in mass was measured for cavitation in LN2, so we can hardly talk about mass loss.

3.4 Other materials

Finally, some commonly used engineering materials were tested (Fig. 11). Specifically, these were: CuZn39Pb3 (Brass), CuSn12 (Bronze), AISI type 304 (Stainless steel), Ti-6Al-4V (Titanium alloy).

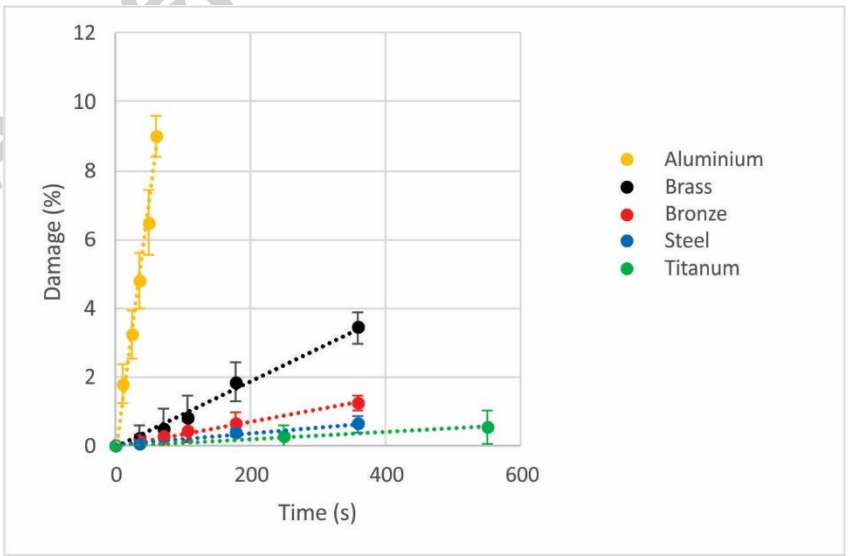

Figure 11: Damage measured in different materials exposed to cavitation at cavitation number σ=9.0, P=338W in LN2.

As expected other (more "engineering") materials performed much better than aluminium 6060. The materials resistance seems to be well related to the surface hardness of the material, what was already found in studies of ultrasonic and hydrodynamic cavitation in waters [25].

4 Discussion

As an assumption we consider here that the bubble number density and the initial bubble radius are the same for the same cavitation number (regardless of the liquid). Hence we can investigate the physics of the phenomenon just by considering one single bubble [26]. We have also shown in our previous work [3] that the approach considering a spherical collapse of a bubble produces a good prediction and interpretation for the influence of the thermal delay on the cavitation aggressiveness. We solve the Rayleigh-Plesset equation, which, for the case of fluids with considerable thermodynamic effect, needs to be modified [2], [23]:

$$\rho_l\left(R\ddot{R}+\frac{3}{2}\dot{R}^2\right)+\Sigma\dot{R}\sqrt{t}\rho_l=p_v-p_\infty+p_{g0}\left(\frac{R_0}{R}\right)^{3\gamma}-\frac{2S}{R}-4\mu\frac{\dot{R}}{R}. \quad (10)$$

R represents the spherical bubble radius, ρ_l is the liquid density, p_v and p_∞ are the vapour and the system pressure, p_{g0} is the initial gas pressure in the bubble, R_0 is the innitial bubble radius, S is the surface tension and μ is the viscosity. Σ was given previously in Eqn. 8.

Franc & Michel [23] derived the expression for the pressure field, in terms of the distance r from the bubble center and the time p(r,t):

$$p(r,t)=(p_\infty-p_v)\left[\frac{R}{3r}\left(\frac{R_0^3}{4R^3}-4\right)-\frac{R^4}{3r^4}\left(\frac{R_0^3}{4R^3}-1\right)\right]+p_\infty. \quad (11)$$

Eqn. 11 exhibits a maximum as soon as the bubble radius becomes smaller than $R=\frac{1}{\sqrt[3]{4}}R_0$. From this one can calculate the maximum pressure in the liquid as [23]:

$$p_{max}(t)=(p_\infty-p_v)\frac{\left(\frac{R_0^3}{4R^3}-1\right)^{4/3}}{\left(\frac{R_0^3}{R^3}-1\right)^{1/3}}+p_\infty. \quad (12)$$

In our calculations, we assumed that the initial bubble nucleus has a radius of 4 μm and is subjected to the sinusoidal pressure field with a frequency of 20kHz. Equilibrium initial conditions were assumed at the beginning of the simulation – the initial gas pressure was calculated by: $p_{g0}=p_{\infty 0}-p_v+\frac{2S}{R_0}$, where $p_{\infty 0}$ is the system pressure before the ultrasonic horn was switched on. The amplitude of the pressure oscillations was calculated from a stagnation pressures based on the velocities gained from Eqn. 6. Investigating various initial nuclei sizes, we concluded that the choice does not influence the general (non-dimensional) outcome of the

calculation – although the bubble dynamics and shock wave magnitudes change significantly, the predicted dependency of the shock wave magnitude on the temperature does not change.

Figure 12 shows the dynamics of cavitation bubble (its radius) in time for liquid nitrogen and water at various conditions, which were investigated experimentally.

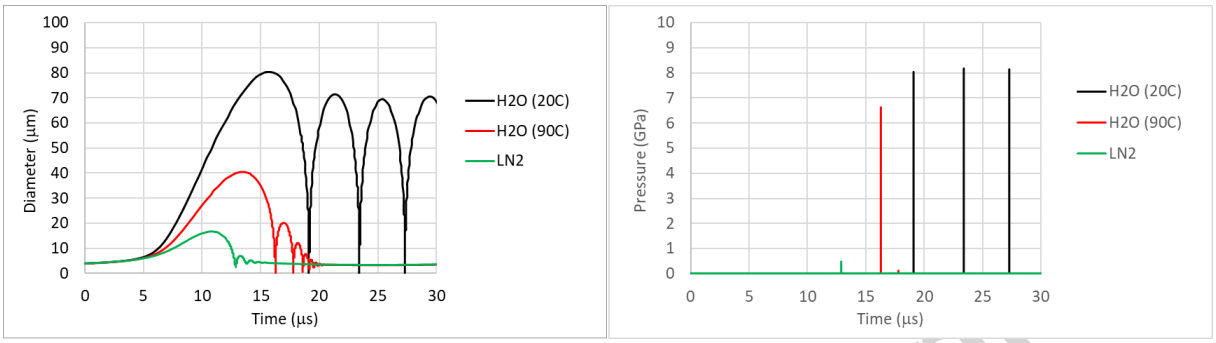

Figure 12: Prediction of the model. Cavitation bubble dynamics (bubble radius, left) and the aggressiveness of bubble collapse (shock wave magnitude, right) for different liquids.

The left diagram shows the influence of the thermodynamic effect on the dynamics of the cavitation bubble. It shows that as the value of parameter Σ (Eqn. 9) increases the bubble size will decrease – known as the delay in the growth of the cavitation bubble – or thermal delay. Somewhat surprising is that the change in the dynamics is almost in the same order between cold and hot water and between hot water and LN2, while the change in Σ is not (Σ = 4ms$^{-3/2}$, 1602ms$^{-3/2}$ and 1925ms$^{-3/2}$ for cold water 20°C, hot water 90°C and LN2, respectively).
The right diagram shows the prediction of the magnitude of the shock wave, which is released at bubble collapse. These vary significantly from 8GPa for cold water to a comparable 6.5GPa for hot water and eventually to only 0.5GPa for LN2. The significant decrease in the predicted magnitude of the shock wave is in sync with the measured trends, where cavitation damage in water was similar regardless of its temperature and was much smaller in the case of LN2 (Figs. 8-10).
While the effect of the collapse velocity is taken into the account by the Rayleigh-Plesset equation another possible reason [27] – the compressibility of the liquid – is not. The sonic velocity in LN2 is significantly lower than in cold (20°C) and hot (90°C) water, where it is comparable 1056 m/s, 1481 m/s and 1550 m/s, respectively. When the bubble collapses at some distance from the wall (specimen), the pressure wave is attenuated by the time (by the distance) it reaches it. Higher compressibility results in higher attenuation, smaller pressure wave amplitude at the wall and consequently smaller erosion rate.
Although questions still remain open, one can conclude that the Rayleigh-Plesset equation, with an added thermodynamic effect term, can be a useful tool for, at least qualitative, prediction of the cavitation aggressiveness in themnosensible fluids.

5 Conclusions

We have performed a series of experiments to deepen the understanding of cavitation erosion in thermosensible fluids. Measurements during the incubation and mass loss periods were performed. Also different engineering materials were tested in LN2, water and hot water

cavitation. It was shown that cavitation in LN2 is much less aggressive than in cold water and even in hot water – a fluid which is many times used as a surrogate to cryogenic liquids.
An important contribution is also our suggestion for a new way to evaluate an acoustic cavitation number (Sec. 2.3), which seems to predict the cavitation appearance well – a much more thorough study of this parameter is foreseen in the future.
Although the change in the hardness of the material specimen as a function of the temperature is significant, it is still not large enough to be the sole reason for minor damage caused by cavitation in LN2. Also, if it were, then the damage at an increased temperature should be large compared to the one at 20°C. The strain rate of deformation could play a role, but it is unlikely that the trend, set according to the surface hardness, would be altered.
Finally, we show that the Rayleigh-Plesset equation with consideration of the thermodynamic effects can be a valuable tool for the prediction of cavitation aggressiveness.

Acknowledgments
The work was performed in the scope of the project "Cavitation and Cavitation erosion in Cryogenic fluids" financially supported by the European Space Agency (ESA).

References

[1] K. Ohira, T. Nakayama, and T. Nagai, "Cavitation flow instability of subcooled liquid nitrogen in converging–diverging nozzles," *Cryogenics*, vol. 52, no. 1, pp. 35–44, Jan. 2012.
[2] M. Dular and O. Coutier-Delgosha, "Thermodynamic effects during growth and collapse of a single cavitation bubble," *Journal of Fluid Mechanics*, vol. 736, pp. 44–66, Dec. 2013.
[3] M. Dular, "Hydrodynamic cavitation damage in water at elevated temperatures," *Wear*, vol. 346–347, pp. 78–86, Jan. 2016.
[4] J. P. R. Gustavsson, K. C. Denning, and C. Segal, "Hydrofoil Cavitation Under Strong Thermodynamic Effect," *Journal of Fluids Engineering*, vol. 130, no. 9, p. 91303, 2008.
[5] J.-P. Franc, G. Boitel, M. Riondet, E. Janson, P. Ramina, and C. Rebattet, "Thermodynamic Effect on a Cavitating Inducer—Part II: On-Board Measurements of Temperature Depression Within Leading Edge Cavities," *Journal of Fluids Engineering*, vol. 132, no. 2, p. 21304, Feb. 2010.
[6] J. Hord, "Cavitation in Liquid Cryogens-II- Hydrofoils," 1973.
[7] J. Hord, "Cavitation in liquid cryogens I - Venturi," *NASA CR-2054*, Jan. 1972.
[8] J. Hord, "Cavitation in liquid cryogens III-Ogives," *NASA CR - 2242*, 1972.
[9] M. Petkovšek and M. Dular, "Observing the thermodynamic effects in cavitating flow by IR thermography," *Experimental Thermal and Fluid Science*, vol. 88, pp. 450–460, Nov. 2017.
[10] M. Petkovšek and M. Dular, "IR measurements of the thermodynamic effects in cavitating flow," *International Journal of Heat and Fluid Flow*, vol. 44, pp. 756–763, Dec. 2013.
[11] R. Garcia and F. G. Hammitt, "Cavitation damage and correlations with material and fluid properties," 1966.
[12] J. R. J. S.G. Young, "Effect of temperature and pressure on cavitation damage to a cobalt base alloy in sodium, Characterization and Determination of Erosion Resistance," *ASTM STP 474, ASTM*, pp. 67–102, 1971.
[13] M. S. Plesset, "Temperature Effects in Cavitation Damage," *Journal of Basic Engineering*, vol. 94, no. 3, p. 559, Sep. 1972.
[14] S. Hattori, I. Komoriya, S. Kawasaki, and S. Kono, "Cavitation erosion of silver plated coatings in a low-temperature environment," *Wear*, vol. 292–293, pp. 74–81, Jul. 2012.
[15] M. Dular, "Hydrodynamic cavitation damage in water at elevated temperatures," *Wear*, vol. 346–347, 2016.

[16] ASTM G32-16, "Standard Test Method for Cavitation Erosion Using Vibratory Apparatus," *ASTM International, West Conshohocken, PA, 2016, www.astm.org*.

[17] K.-H. Kim, G. Chahine, J.-P. Franc, and A. Karimi, Eds., *Advanced Experimental and Numerical Techniques for Cavitation Erosion Prediction*, vol. 106. Dordrecht: Springer Netherlands, 2014.

[18] ASTM E10-15, "ASTM E10-15 Standard test method for Brinell hardness of metallic materials," *ASTM International, West Conshohocken, PA, 2015, www.astm.org.*

[19] G. L. C. Jean-Pierre Franc, Michel Riondet, Ayat Karimi, "Material and velocity effects on cavitation erosion pitting," *Wear*, vol. 274–275, pp. 248–259, Jan. 2012.

[20] A. Žnidarčič, R. Mettin, C. Cairós, and M. Dular, "Attached cavitation at a small diameter ultrasonic horn tip," *Physics of Fluids*, vol. 26, no. 2, p. 23304, Feb. 2014.

[21] B. Dular, M., Sirok, B., Stoffel, "The influence of the gas content of water and the flow velocity on cavitation erosion aggressiveness," *J. mech. eng.*, vol. 51, no. 3, pp. 132–145, 2005.

[22] M. Dular, B. Bachert, B. Stoffel, and B. ?irok, "Relationship between cavitation structures and cavitation damage," *Wear*, vol. 257, no. 11, 2004.

[23] J.-P. Franc and J.-M. Michel, *Fundamentals of cavitation*. Kluwer Academic Publishers, 2004.

[24] S. Hattori, K. Taruya, K. Kikuta, and H. Tomaru, "Cavitation erosion of silver plated coatings considering thermodynamic effect," *Wear*, vol. 300, no. 1–2, pp. 136–142, Mar. 2013.

[25] M. Yokota, H. Mochizuki, and T. Hirano, "Cavitation Erosion of Pure Titanium TB340C and Stainless Steel SUS316 in Seawater," *Journal of The Japan Institute of Marine Engineering*, vol. 44, no. 3, pp. 442–447, 2009.

[26] J.-P. Franc, "The Rayleigh-Plesset equation: a simple and powerful tool to understand various aspects of cavitation," Springer, Vienna, 2007, pp. 1–41.

[27] M. Dular, B. Stoffel, and B. ?irok, "Development of a cavitation erosion model," *Wear*, vol. 261, no. 5–6, 2006.

Highlights

- Cavitation in LN2 is considerable less aggressive than in water
- Cavitation aggressiveness in hot and cold water are comparable
- Acoustic cavitation number is proposed
- Extended Rayleigh-Plesset equation can provide a good prediction